AAS 11-418

MITIGATING POTENTIAL ORBIT DEBRIS: THE DEORBIT OF A COMMERICAL SPACECRAFT

Timothy Craychee*, Shannon Sturtevant†

In the spring of 2011, a commercial spacecraft (SSC Object #27838) performed a final maneuver that sent the spacecraft into Earth's lower atmosphere resulting in a reentry event that began over the southern Pacific Ocean. While it is not known if any spacecraft debris survived reentry, the design of the final orbit was such that potentially surviving debris would impact within a "safe zone" in the Pacific Ocean. The purpose of this paper is to report the deorbit trajectory design and implementation, which includes accommodating constraints and limitations of a vehicle whose design and mission never included a controlled deorbit.

INTRODUCTION

In 2010, a decision was made to perform a controlled reentry of a polar orbiting commercial satellite SSN #27838. This decision was prompted by the fact that the satellite's primary mission terminated in 2007 and the ground system being used to maintain contact with the vehicle was slated to be decommissioned. Instead of abandoning a functioning and commandable satellite in an orbit that would take years to naturally decay, posing an ongoing conjunction threat to other space objects and potentially exacerbating the increasing density of objects in the space environment, a decision was made to command a controlled deorbit of the satellite. However, it is significant to note that there was no mission or regulatory requirement to perform a controlled deorbit and the vehicle was not designed to support such an activity. Thus, there were many ground and space system limitations and constraints that needed to be accommodated as part of the successful execution of this controlled reentry. These factors, along with other requirements and guidelines, influenced the overall trajectory design and implementation. This paper presents both the original deorbit design as well as its evolution throughout execution.

INITIAL DEORBIT DESIGN

With the spacecraft nominal mission ending in March of 2007, the spacecraft continued to orbit without any maintenance maneuvers. This left the vehicle in a slightly decayed orbit from that of its original mission. The orbital parameters incorporated into the original deorbit design were obtained from a two-line element from CelesTrak[1] and are illustrated in Table 1.

* Senior Aerospace Engineer, Space Group, Applied Defense Solutions, 8171 Maple Lawn Blvd Fulton MD 20759
† Senior Mission Analyst, Independent, 3560 Otis St, Wheat Ridge, CO 80033.

Table 1. Initial Kozai-Izsak Mean Elements Derived from TLE

Elements	Initial Design State
Epoch (UTCG)	1/5/2011 12:00
Mean_Semimajor_Axis (km)	6808.404112
Mean_Eccentricity	0.001124
Mean_Inclination (deg)	97.034
Mean_RAAN (deg)	53.003
Mean_Argument_of_Perigee (deg)	83.149
Mean_True_Anomaly (deg)	6.351

Because initial orbit parameters identified the vehicle at an altitude above the International Space Station (ISS), the deorbit was designed to have two phases, referred to as Phase 1 and Phase 2 from here forward. Phase 1 was designed to lower the spacecraft to an approximately circular orbit with a mean radius below that of the ISS. Phase 2 followed and was designed to lower the periapsis altitude such that a reentry occurred with a specific impact location in the Pacific Ocean (detailed below).

The design utilized six burn activities for Phase 1 and five burn activities for Phase 2. Two days were incorporated between each maneuver to allow time for telemetry collection and analysis, burn calibration, and updates to future maneuver plans.

The two phase approach was a conservative strategy designed so that if, due to some unknown factor, any of the maneuver activities happened to be the last, the spacecraft would not be an immediate threat to another space object, with utmost attention given to the manned ISS. Once the design was finalized, the proposed deorbit plan was then submitted to regulatory agencies for government approval, which it received. The following sections provide more detail on each phase as designed.

Phase 1 Design

The Phase 1 design consisted of six burn activities. The first two were test activities including a checkout with a zero second burn duration and a 30 second calibration maneuver. The intention of the zero second maneuver was to test the command load generation procedure as well as to ensure that the spacecraft behavior matched simulation results. The calibration burn was designed to validate and finalize assumptions in models being used for maneuver planning, specifically those associated with the propulsion model. The remaining four activities were the primary burns used to lower the entire spacecraft orbit below that of the ISS, each with a 300 second burn duration. The reasons for implementing this approach were twofold:

- Minimize the time the spacecraft spends in an ISS crossing orbit.
- Adhere to an onboard constraint limiting maximum burn duration to 300 seconds.

Since the spacecraft's orbital radius would necessarily cross the ISS orbit no matter the deorbit strategy, the decision was made to lower the entire orbital radius below that of the ISS. This ensured that at the end of Phase 1 the spacecraft would no longer have the potential to conjunct with the ISS. However, an early-identified operational constraint required multiple burns to achieve this goal. In the earliest examination of the feasibility of a controlled deorbit of this vehicle, an onboard constraint was identified that limited the maximum commandable burn duration to 300

seconds. Therefore, circularization below the ISS required a four burn sequence following the two test activities of Phase 1.

The Phase 1 design is illustrated in Figure 1 and Figure 2. Figure 1 is a comparison of the orbit radii of the spacecraft and the ISS. Included in the figure are the four 300 second maneuvers that complete Phase 1. Upon completion of the third maneuver in the figure, the spacecraft and the ISS orbital radii overlap until the following maneuver, after which the orbital radii would no longer overlap.

Since the Phase 1 design included an overlap between the spacecraft and the ISS, the design utilized the synodic period between the two objects as a constraint. The synodic period is defined as the relative orbit period between the spacecraft and ISS. The first three maneuvers of Figure 1 increased the synodic period to over 100 days when the orbital radii overlap would occur (see Figure 2). This would allow for ample reaction time if an anomaly were to occur.

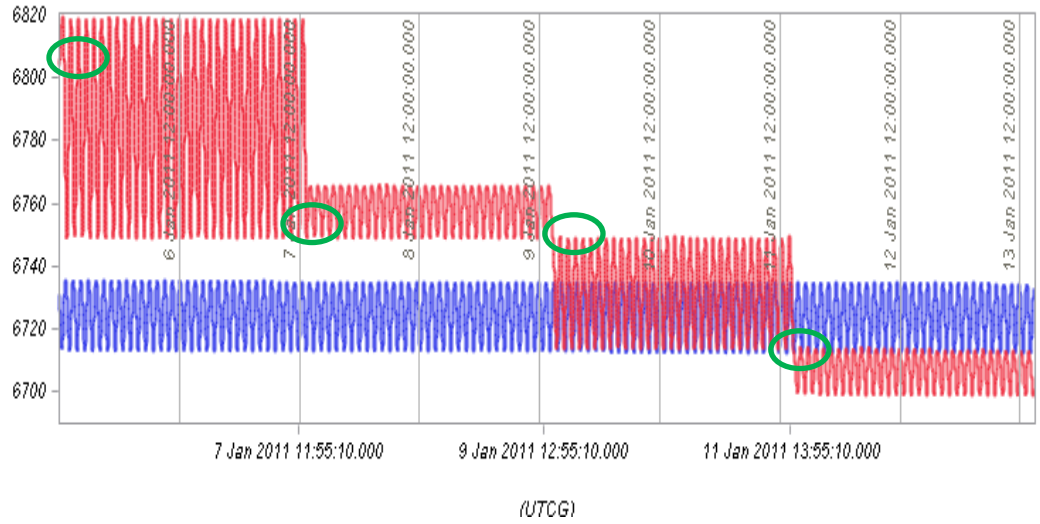

Figure 1. Phase 1 Design: Spacecraft (red) and ISS (blue) Orbit Radii in km

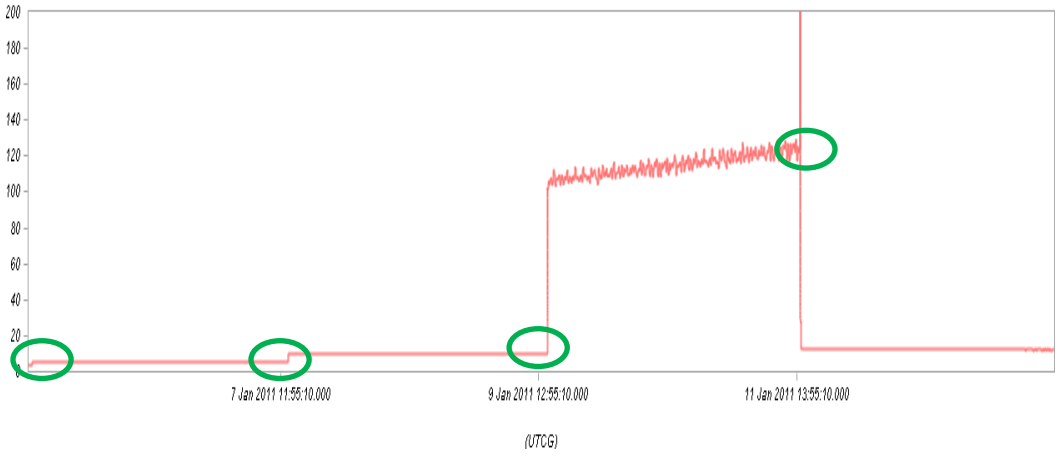

Figure 2. Phase 1 Design: Synodic Period between Spacecraft and ISS in days

Phase 2 Design

The Phase 2 design utilized five maneuvers to lower the orbit periapsis to reentry and also to align the impact area to the desired location, described in detail below. NASA-STD 8719.14[2] was only used as a guideline for the Phase 2 design. The standard states:

> "If the amount of debris surviving reentry exceeds the requirement, then either the ground impact point is modified by a post mission disposal maneuver or measures are taken to reduce the amount of debris surviving reentry. Options to consider include:
>
> a. Performing a controlled reentry. Maneuver the structure at EOM to a reentry trajectory with an effective perigee altitude no higher than 50 km to control the location of the reentry and ground impact points (see Section 4.6)."

Since a survivability analysis had not been performed, the trajectory was conservatively designed to lower the periapsis altitude to 50 km where a controlled reentry event would occur due to the drag force induced by Earth's atmosphere.

Phase 2 was still mostly designed to work within the confines of the 300-second burn duration limit however it was assumed that the onboard constraint would be increased prior to the final maneuver. The flight dynamics team was committed to revising the onboard limit so that the departure periapsis for the final burn could be maximized. This was desired to reduce risk associated with attitude control at low perigee altitudes. In addition, unlike Phase 1, Phase 2 maneuvers were designed to target specific post-maneuver periapsis altitudes that incrementally stepped the vehicle toward reentry. Targeting altitudes allowed flexibility in the overall deorbit design such that perturbations and uncertainties during operations could be easily absorbed by burn duration, which would be allowed to vary in subsequent maneuver planning. The design also allowed for the spacecraft state and heath to be evaluated in stages as it dipped deeper into the Earth's atmosphere. Maneuver timing was also a significant component of Phase 2 since the timing of the first maneuver was used to rotate the line of apsides to set the desired impact location, which also affected the burn durations required by the following maneuvers. The effect of the Phase 2 maneuvers on the orbital radius of the spacecraft can be seen in Figure 3.

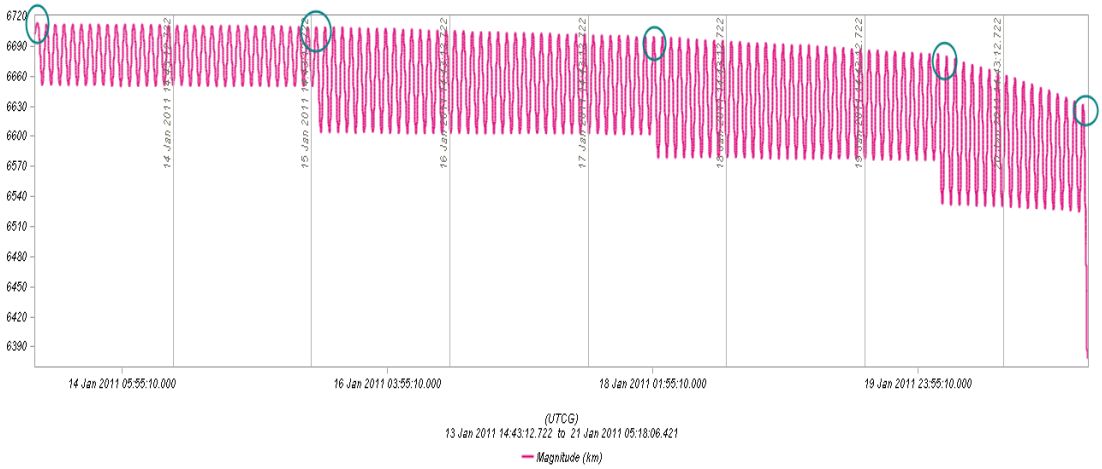

Figure 3. Phase 2 Design: Spacecraft Orbit Radius in km

A complete list of the Phase 1 and Phase 2 primary maneuvers as designed is shown in Table 2.

Table 2. Deorbit Design Maneuver Summary (Excluding Checkout and Calibration)

Maneuver Number	Start Time (UTCG)	Stop Time (UTCG)	Duration (sec)	Delta V (m/sec)	Fuel Used (kg)
1	1/5/2011 12:42	1/5/2011 12:47	300	15.553715	2.027
2	1/7/2011 13:22	1/7/2011 13:27	300	15.074523	1.954
3	1/9/2011 14:32	1/9/2011 14:37	300	14.645088	1.889
4	1/11/2011 14:37	1/11/2011 14:42	300	14.257949	1.83
5	1/13/2011 15:14	1/13/2011 15:19	300	13.907042	1.776
6	1/15/2011 15:32	1/15/2011 15:37	300	13.587404	1.727
7	1/18/2011 2:04	1/18/2011 2:07	150	6.68247	0.846
8	1/20/2011 3:21	1/20/2011 3:26	298.503	13.092829	1.652
9	1/21/2011 4:28	1/21/2011 4:40	671.34	28.542039	3.574
		Totals:	2919.843	135.343058	17.274

Preliminarily Identified Contingencies

As part of the design phase, preliminary contingencies were identified along with steps necessary to address them if possible. Those contingencies were:

- The inability to perform maneuvers
- Loss of X-Band communications capability
- Loss of spacecraft attitude control (tumble event)

In the event that the spacecraft was unable to perform subsequent maneuvers, the flight dynamics team imposed planning requirements to ensure risk to other spacecraft was minimized. The first requirement was to screen each maneuver plan for conjunctions up to four days following execution. If a conjunction of concern was identified, the maneuver plan would be adjusted to mitigate the event. . In addition, as explained above, Phase 1 was designed to minimize the conjunction threat to the ISS.

Early involvement with spacecraft operations preceding the deorbit identified a possible communication vulnerability. The spacecraft had two forms of communicating with the ground, an X-Band antenna (primary) and a UHF antenna (secondary). Occasionally, the X-Band communications would be lost and the spacecraft would switch to the UHF antenna. Experience showed that X-band could be recovered fairly quickly; however, steps were taken to improve the efficiency of the UHF downlink ensuring that the majority of the data needed would be available.

Lastly, loss of attitude control during the deorbit was identified as a possibility. The spacecraft's attitude control system included torque rods and four reaction wheels, one on each primary axis and one askew to all three axes. In the event that one or more of these wheels became saturated due to high torques on the vehicle, such as those expected in the increasing atmospheric drag environment of Phase 2, the spacecraft could succumb to an unrecoverable tumble. If this were to happen, deorbit operations would cease. The flight dynamics team identified two strategies to address this issue. The first involved analyzing the utility of a low-drag flight profile during times when the spacecraft would encounter the highest drag environment. Early analysis showed that implementing the low drag profile increased the ability of the vehicle to retain control throughout the high drag periods. The second, mentioned above, was to revise the onboard burn duration limit to maximize the departure periapsis for the final burn.

REENTRY REQUIREMENTS AND IMPACT AREA SELECTION

In order to perform a controlled deorbit, the location of the reentry and ground impact points had to be selected. Again, the NASA-STD 8719.14[2] was used for guidance. The standard states:

> "For controlled reentry, the selected trajectory shall ensure that no surviving debris impact with a kinetic energy greater than 15 joules is closer than 370 km from foreign landmasses, or is within 50 km from the continental U.S., territories of the U.S., and the permanent ice pack of Antarctica (Requirement 56627)."

Based on analysis, there are three zones that meet these criteria in the Atlantic, Pacific, and Indian Oceans. Of these three, the Pacific Ocean zone is the largest. Figure 4 depicts the allowable impact zone used for planning this activity with boundaries at least 700 km from the nearest land mass, exceeding the NASA-STD 8719.14[2] requirements.

Figure 4. Allowable Pacific Impact Region

Since a break-up analysis was not performed, the flight dynamics team conducted a monte carlo analysis of potentially surviving debris in order to predict the impact location. This analysis examined the effects of maneuver execution errors and breakup uncertainties on the final maneuver burn duration and impact location. The maneuver execution errors were modeled as perturbations in terms of thrust efficiency as well as pointing errors. The monte carlo perturbs individual maneuvers while still performing the remaining maneuvers to determine if the trajectory goals are still met.

The monte carlo utilizes Gaussian distributions for the maneuver magnitude error (thrust efficiency) and maneuver direction, where the three sigma value is six percent and one degree respectively. Additionally, the monte carlo modeled break-up uncertainties as a function of ballistic coefficient.

The monte carlo executed 1000 cases with all 1000 cases impacting within the allowable area shown in Figure 4. The precise impact location of each case is shown in Figure 5. The latitude and longitude values were then analyzed to determine the footprint of the 3-sigma impact ellipsoid[3]. The size of the footprint is determined using Equation 1 and Equation 2. In the equations the

parameter "A" varies from 0 to 2π in steps of five degrees as depicted in Figure 5. The resulting ellipse has a semi-major axis of 761 km and a semi-minor axis of 721 km and encompasses all Phase 1 and 2 activities.

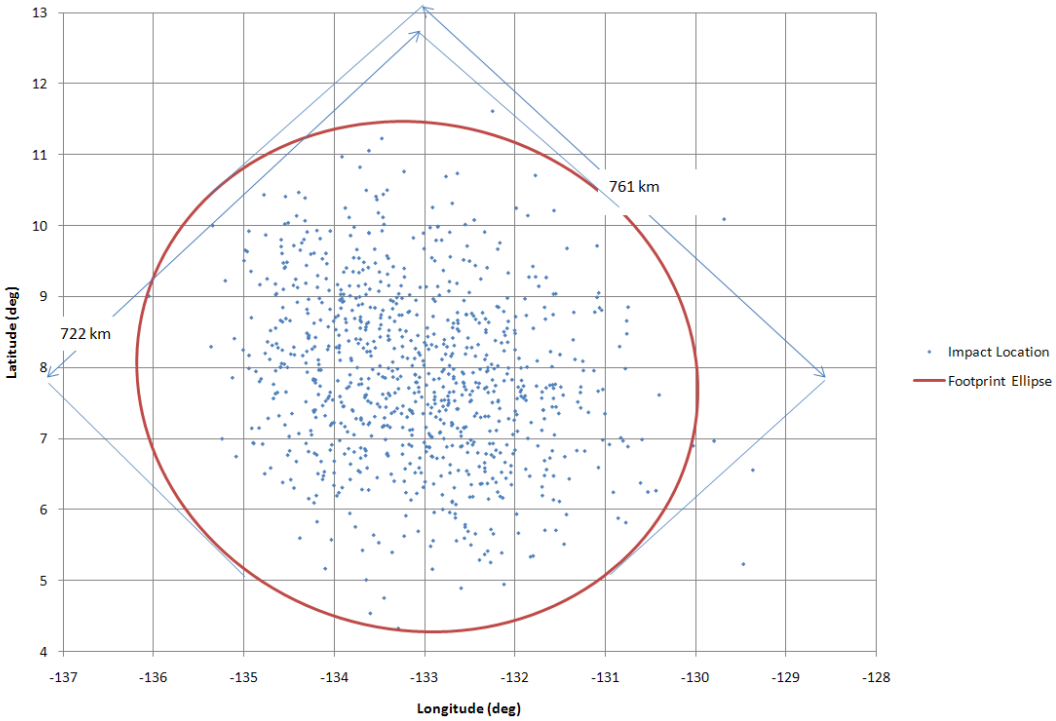

Figure 5. Monte Carlo Impact Locations and 3-sigma Ellipsoid

$$Ellipse_{Lat} = Latitude_{Mean} + Latitude_{StdDev} * Cos(A) * Cos(Clock\ Angle) - Longitude_{StdDev} * Sin(A) * Sin(Clock\ Angle) \quad (1)$$

$$Ellipse_{Lon} = Longitude_{Mean} + Latitude_{StdDev} * Cos(A) * Sin(Clock\ Angle) - Longitude_{StdDev} * Sin(A) * Sin(Clock\ Angle) \quad (2)$$

MANEUVER OPERATIONS

The following sections detail the actual execution of the deorbit including changes to the trajectory design and challenges encountered along the way.

Phase 1 Execution

Phase 1 consisted of seven maneuver activities, one more than in the design. The difference was the addition of a collision avoidance (COLA) maneuver following the checkout and calibration activities. Another change from design was that the four primary burns were changed from 300 seconds in duration to 296 seconds. With a better understanding of vehicle commanding, Eq-

uation 3 was used to determine the maximum commandable burn duration related to the 300 second burn duration constraint. The results of these maneuvers are shown in Table 3.

$$Max\ Commandable\ Burn\ Duration = (Max\ Burn\ Duration\ Constraint) - (Max\ Burn\ Duration\ Constraint) * (2\%\ margin) + (2\ Second\ Automatic\ Cuoff\ Delay) \quad (3)$$

Table 3. Phase 1 Maneuver Results

Maneuver	Ignition Time (UTCG)	Burn Duration (sec)	Fuel Usage (kg)	Maneuver Goal	Periapsis Alt. (km)	Apoapsis Alt. (km)	Thrust Eff. (%)	Total Fuel Remaining (kg)
Initial State	----------	--------	----------	----------	421.9619479	439.1203476	--------	23.837
Calibration Burn	22 Dec 2010 12:52:34.200	30.34775	0.1895	Lower Perigee	416.7681586	439.1076402	93.3	23.6475
COLA Mnvr	02 Jan 2011 06:50:32.887	30.01675	0.186699	Lower Perigee	411.598784	438.78833	94.6	23.460801
Maneuver 1	05 Jan 2011 12:27:50.361	287.705	1.8034532	Lower Perigee	363.0832021	438.311241	92.09	21.657348
Maneuver 2	07 Jan 2011 13:05:49.722	287.7125	1.7469524	Lower Apogee	363.3818341	390.5161209	92.164	19.910395
Maneuver 3	09 Jan 2011 14:15:51.466	286.3125	1.6858694	Lower Apogee	343.7927444	364.0438907	91.727	18.224526
Maneuver 4	11 Jan 2011 17:18:25.000	--------	----------	Lower Apogee	----------	----------	--------	----------

The checkout and calibration activities performed exactly as expected based on documentation obtained through research. The maneuver planning was done such that mismodeled parameters could be accounted for and revised quickly without significant impact to the overall de-orbit plan. As part of this design, the calibration maneuver plan assumed a 100% efficiency to ensure that the maneuver was not being biased during the planning stages, even though documentation suggested that the efficiency would approximately be 93%. Actual post-burn calibration, detailed below, resulted in an efficiency of 93.3% verifying the documentation. Calibrated efficiency values were then used for subsequent planning as illustrated in Table 3.

The COLA maneuver was performed to avoid a piece of Delta-1 debris, SSN 9617. The flight dynamics team used this maneuver to contribute to the deorbit efforts and matched the burn duration to that of the calibration burn. This resulted in a larger than required COLA maneuver but allowed the flight dynamics team to verify the thruster efficiency value of 93.3% obtained from the calibration maneuver.

Figure 6 shows the affects of the calibration and COLA maneuvers. Both maneuvers occurred at apoapsis, lowering periapsis.

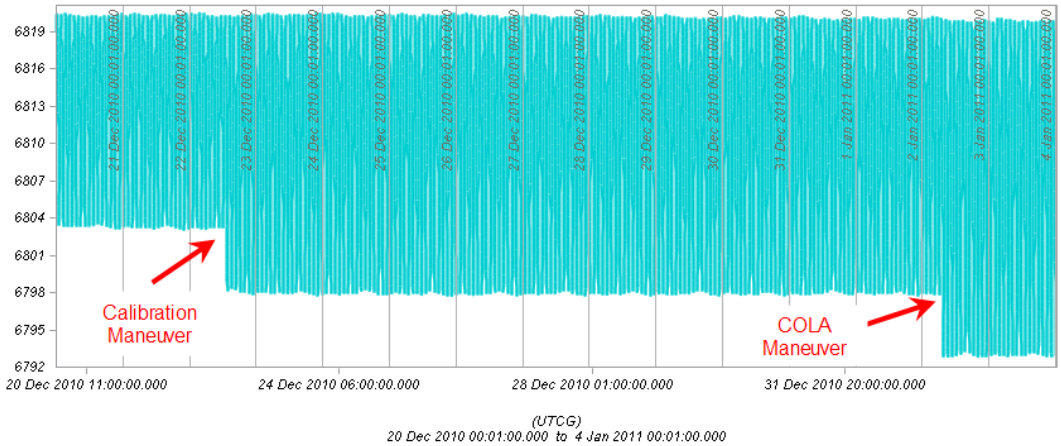

Figure 6. Orbit Radius Change Due to Calibration & COLA Maneuvers

The four primary maneuvers of Phase 1 continued to lower the spacecraft, via a series of apoapsis and periapsis maneuvers, to an orbital radius below that of the ISS. Two of the four maneuvers, conducted specifically at periapsis, lowered the orbital radius such that once the maneuver had completed, the pre-maneuver periapsis location became the post-maneuver apoapsis location. Figure 7 illustrates this.

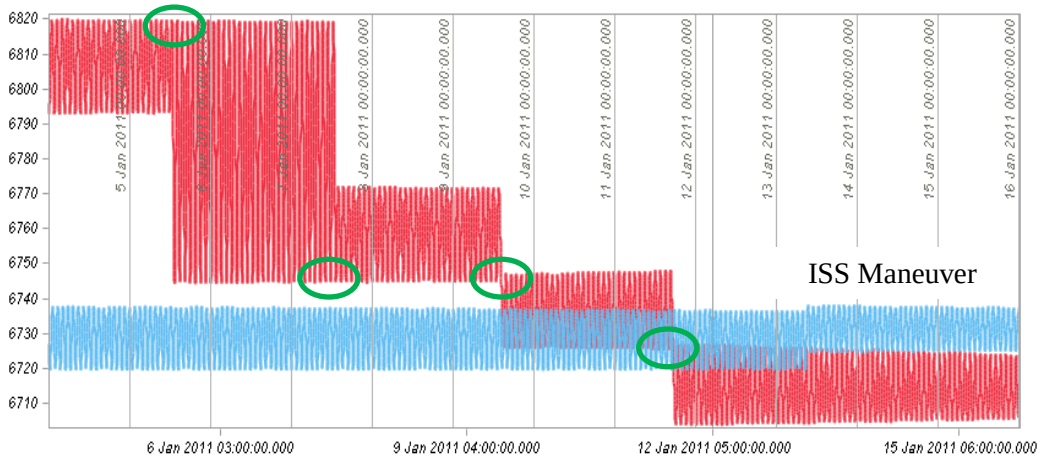

Figure 7. Phase 1 Execution: Spacecraft (red) and ISS (blue) Orbit Radii in km

As per the design the second to last maneuver of Phase 1 put the spacecraft into an orbit with a radius that overlapped that of the ISS. This maneuver increased the synodic period from approximately 10 to 150 days (Figure 8), well over the design goal of 100 days.

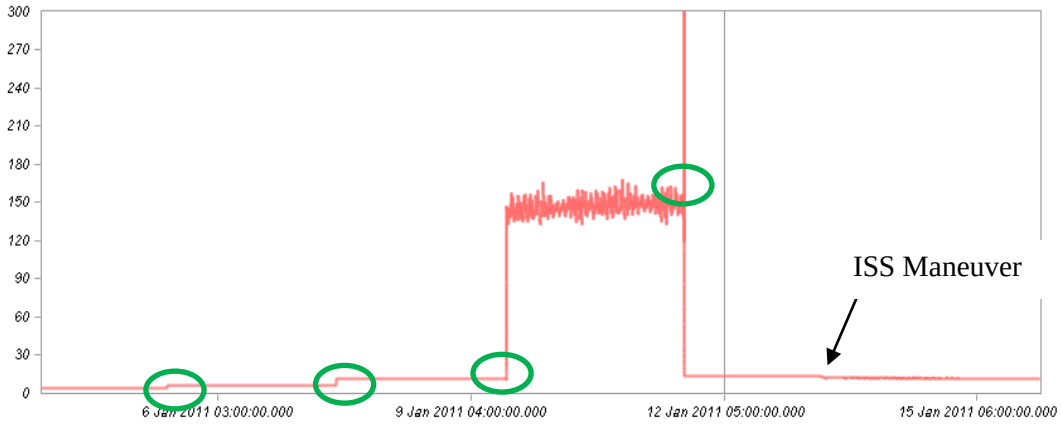

Figure 8. Phase 1 Execution: Synodic Period between Spacecraft and ISS in days

For Phase 1 the main difference between the design and the actual maneuvers was due to maneuver performance. The design utilized a performance value of 100%, which was expected to change based on performance data. Following execution, the maneuver spacing allowed the actual maneuvers to be analyzed. Analysis results revealed a performance of about 92-93% due to thruster off pulsing. This was accounted for by updating the trajectory plan along the way to ensure that the final burn of Phase 1 would successfully lower the spacecraft below the ISS. In addition, a scheduled maneuver that boosted the ISS orbit contributed to successful completion of Phase 1.

Phase 2 Revision

The design of Phase 2 consisted of a total of five maneuvers, approximately two days apart, with the final maneuver lowering the periapsis from 150 km to 50 km. Using the maneuver performance values derived during the execution of Phase 1 along with enhanced understanding of the vehicle capabilities gained from additional research and analysis during the Phase 1 activity, the Phase 2 execution changed significantly from the design. There were four major items that arose during the activity that needed resolution before initiating the execution of Phase 2:

- Adjusting the onboard maximum burn duration constraint
- Determining the maximum burn duration for which the spacecraft could maintain attitude control
- Identifying the trajectory of the final maneuver including:
    - minimum altitude of the last maneuver based on the ability of the spacecraft to maintain attitude control through low altitude perigees
    - post-final-maneuver periapsis altitude
- Revising the impact location after changing above items

Adjusting the Onboard Maximum Burn Duration Constraint

Investigations during the activity revealed that the onboard maximum burn duration limit could be adjusted via a flight parameter upload. The limit of 300 seconds did not impact the operations of Phase 1 but if left unchecked, limited the options available in Phase 2. Therefore, so as not to impose an artificial constraint on the activity, a decision was made to perform a parameter upload changing the constraint from 300 to 2400 seconds, the maximum burn duration the thruster hardware could support as stated by the vendor. This parameter change led to the first changes to the Phase 2 design. It was decided to increase the duration of the first burn of Phase 2 to 350 seconds to validate the onboard change. Assuming validation, it was then decided to use a large enough burn duration so that the second burn would reduce the periapsis to 200 km. This altitude was chosen to be a checkout location where telemetry would be collected and analyzed. These changes also reduced the number of burns required to complete Phase 2 by one.

Determining the Maximum Controllable Burn Duration

Based on telemetry analysis during Phase 1, it became apparent that attitude control during burns longer than 300 seconds may be a concern. During a maneuver, the spacecraft controlled pitch and roll (about the X and Y) body axis via thruster off-pulsing but utilized the reaction wheels for yaw control about the body-Z axis. Telemetry showed that when the thrusters fired, the Z axis reaction wheel speed grew in magnitude from its nominal steady state value as exemplified in Figure 9.

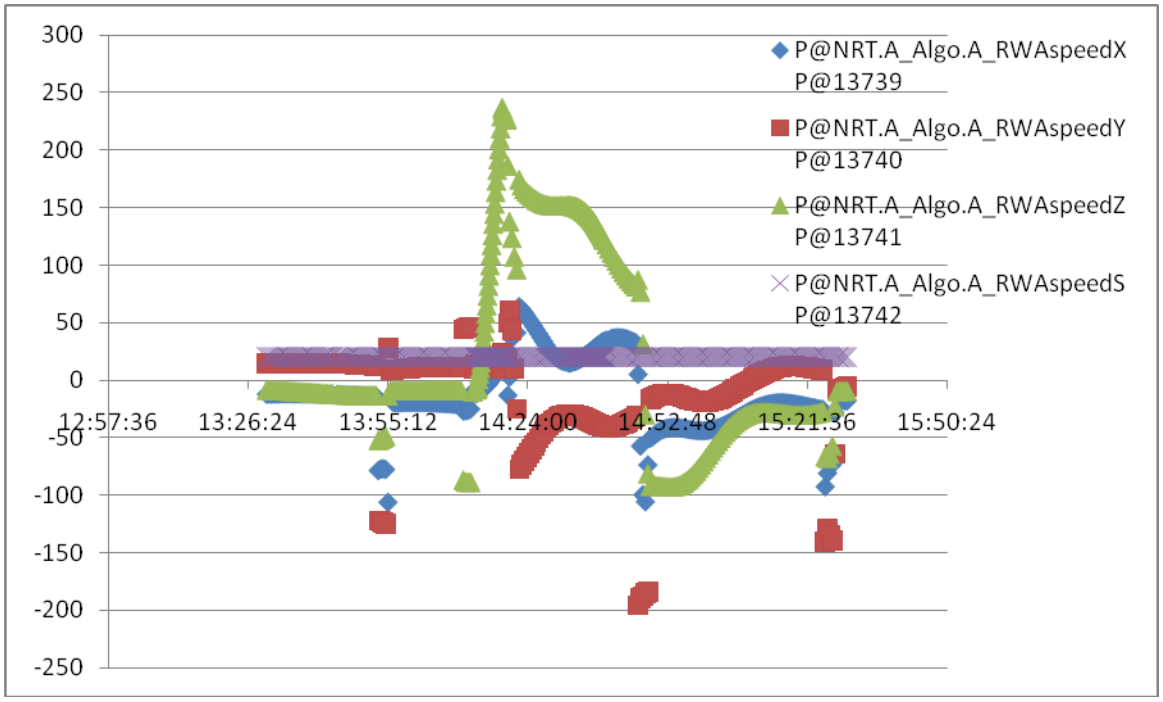

Figure 9. Deorbit Maneuver 3 Reaction Wheel Speeds (rad/s)

Examination of the data showed the Z-wheel speed grew almost linearly during each maneuver. The assumption of linear growth was applied to all available maneuver data to calculate an average growth rate shown in Table 4. In addition, a time lag appeared in the data, where the Z-wheel-speed growth extended beyond the commanded maneuver duration requiring the use of a burn duration multiplier of 1.05. Therefore the Z- wheel-speed growth rate and the change in Z-wheel speed over a maneuver could be determined by Equation 4 and Equation 5.

Table 4. Z-Wheel-Speed Growth During Maneuvers

Maneuver Number	Start Time	Stop Time	Duration (sec)	Starting Z Axis Value (rad/s)	Stopping Z Axis Value (rad/s)	Change in Wheel Speed (rad/s)	Growth Rate ((rad/s)/s)
1	12:27:46	12:32:56	310	-8.89	253.953	262.843	0.847
2	13:06:16	13:11:26	310	-9.171	258.922	268.09388	0.8648
3	14:13:36	13:18:46	310	-8.3125	236.234	244.5465	0.788
					Average:	258.49446	0.8332667

$$Wheel\ Growth\ Rate = (Change\ in\ Wheel\ Speed)/Duration \quad (4)$$

$$Z\ Wheel\ Final\ Speed = (Burn\ Duration * Burn\ Duration\ Multiplier) * (Wheel\ Growth\ Rate) + Z\ Wheel\ Starting\ Speed \quad (5)$$

The reason this was a concern is that Z-wheel speeds projected over maneuvers longer than 300 seconds approached hardware limitations of the reaction wheels. In an attempt to improve this situation, an investigation began into the possibility of changing onboard reaction-wheel-

speed limits as well as using the skew-wheel to bias the initial steady state value of the Z-wheel to allow for more growth.

Figure 10 shows the maximum possible reaction wheel speed as a function of power and temperature of the reaction wheel assembly. Based on the observed temperature and power levels of the vehicle, a conclusion was made that the wheels could achieve approximately 450 rad/s before saturation. Thus, in an attempt to leverage the maximum capacity of the reaction wheels, conservative onboard safety limits where adjusted to accommodate the demanding use.

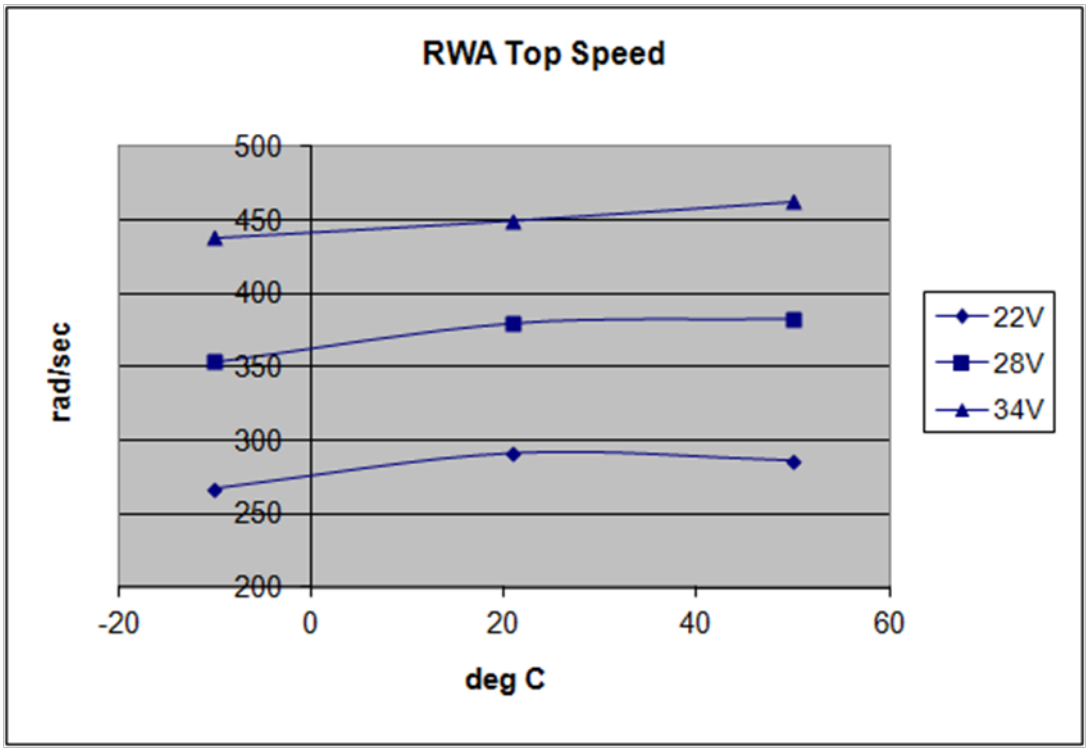

Figure 10. Reaction Wheel Unit Test Data: Top Wheel Speed Based on Battery Voltage and Temperature

In addition to the onboard limit adjustments the skew reaction wheel was used to bias the steady state Z-wheel speed. The skew wheel was commandable and could be used to inflict a torque on the spacecraft that the remaining three wheels were required to counter to maintain a zero momentum system. The orientation of the reactions wheels (see Figure 11) showed that, if the skew wheel was commanded to a positive value, the Z-wheel reacted in the opposite direction.

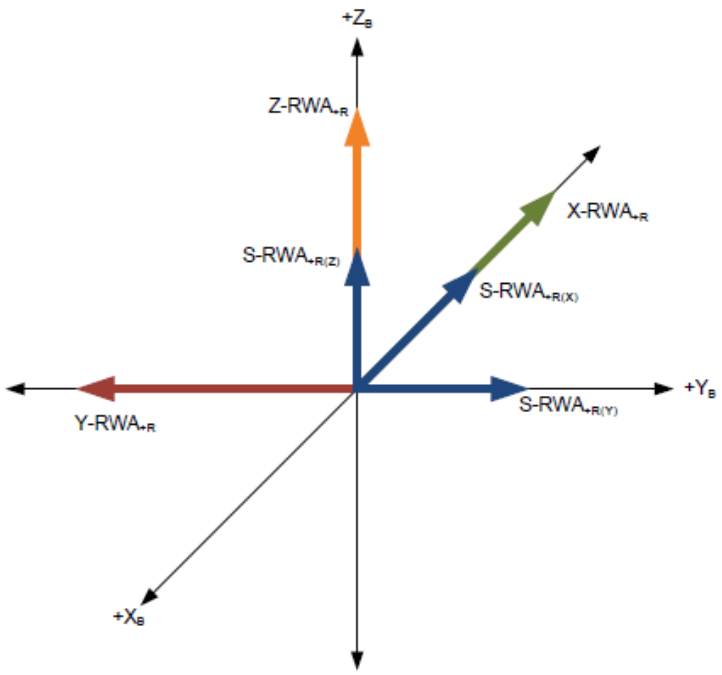

RWA	Z_R Vector Orientation in B-frame		
	X_B Component	Y_B Component	Z_B Component
X-RWA	-0.999989359	-0.004464100	-0.001168534
Y-RWA	-0.000392899	-0.999967302	-0.008079991
Z-RWA	-0.000028102	-0.007335945	0.999973110
S-RWA	-0.608913450	0.612375690	0.504269651

Figure 11. Reaction Wheel Directions and Components

Utilizing the Z-wheel growth rate, the estimated maximum achievable wheel speed, and the skew wheel bias, a burn duration that corresponded to wheel saturation could be calculated, which was used as the maximum commandable duration with reliable attitude control. The following equations and assumptions were used:

- Maximum commandable skew wheel speed: 375 rad/s (conservatism included)
  - This value is the maximum speed expected during nominal operation and was chosen to be conservative; the intention was to rely on nonstandard performance from only the Z-wheel.
- Maximum achievable Z wheel speed: 450 rad/s (conservatism included)
- The final burn does not need the 1.05 multiplier
  - After the final burn the vehicle's attitude stability is no longer a concern.

$$Z\ Wheel\ Starting\ Speed = -Skew\ Wheel\ Speed * 0.504269651$$

$$Z\ Wheel\ Starting\ Speed = -375\left(\frac{rad}{s}\right) * 0.504269651 = -189.10\frac{rad}{s}$$

$$Delta\ Wheel\ Speed = Max\ Achievable\ Wheel\ Speed - Z\ Wheel\ Starting\ Speed$$

$$Delta\ Wheel\ Speed = 450\left(\frac{rad}{s}\right) - \left(-189.10\left(\frac{rad}{s}\right)\right) = 639.10\ \left(\frac{rad}{s}\right)$$

$$Maximum\ Burn\ Duration = \frac{Delta\ Wheel\ Speed}{Wheel\ Growth\ Rate * Burn\ Duration\ Multiplier}$$

$$Maximum\ Burn\ Duration\ (no\ multipler) = \frac{639.10\left(\frac{rad}{s}\right)}{0.8332667\frac{\frac{rad}{s}}{s}} = 766.981\ \text{sec}$$

It was decided that the maximum burn duration value would be rounded down to 750 seconds to be conservative.

Identifying the Trajectory of the Final Maneuver

Once the maximum controllable burn duration had been determined, the remaining trajectory constraints were the departure altitude (i.e. the periapsis altitude of the orbit prior to the maneuver) and the impact location. The initial deorbit design had the fifth and final maneuver of Phase 2 lower the periapsis from 150 km to 50 km to meet objectives. This occurred two days after the fourth maneuver. However, based on a better understanding of the limitations of the attitude control system, concerns also began to arise related to the spacecraft's ability to counter the torque resulting from the high-atmospheric-density, low-periapsis portion of the orbit. To better understand the vehicle capabilities, the spacecraft manufacturer ran a simulation to estimate the likelihood of the spacecraft being able to survive the perigee pass of an orbit with a 300 km apoapsis and 150 km periapsis. Simulation results of 100 runs gave the spacecraft an 85% chance of maintaining control through this period of time. Thus, a choice was made to reduce the amount of time that would occur between the final two maneuvers from two orbits to two days. This reduced the time that the spacecraft would spend in the highest drag environment it would experience before reentry. In addition, it was clearly desirable to raise the departure altitude above 150 km by as much as possible. The maximum controllable burn duration remained a significant constraint but a decision was made to allow the final periapsis altitude to vary. The 50 km target periapsis was an ideal value but past experience allowed the flight dynamics team to be comfortable with a value of 70 km. This resulted in a variety of trajectory options that were examined (see Table 5). The options varied the duration and the periapsis departure altitude of the final maneuver. The resulting impact point (latitude and longitude) as well as final periapsis altitude were then evaluated.

Table 5. List of Design Cases for Phase 2

Case Name	Departure Altitude (km)	Burn Duration (sec)	Impact Latitude (deg)	Impact Longitude (deg)	Final Perigee Altitude (km)	Notes
Current Nominal	150	801	7.829	-136.534	50.002	
D150B800	150	800	7.898	-136.547	50.108	Most Desired - Lowest Depart, Longest Burn Duration
D150B750	150	750	11.688	-137.250	55.746	Desirable - Lowest Depart, Long Burn Duration
D150B700	150	700	16.091	-138.082	61.479	Desirable - Lowest Depart
D150B600	150	600	27.900	-140.470	73.217	Undesirable - Low Depart, High Per Alt
D160B800	160	800	14.592	-137.851	59.578	Desirable - Low Depart, Longest Burn Duration
D160B750	160	750	19.415	-138.783	65.249	Desirable - Low Depart, Long Burn Duration
D160B700	160	700	25.311	-139.976	71.017	Desirable - Low Depart
~~D160B600~~	~~160~~	~~600~~	~~43.861~~	~~-144.494~~	~~82.827~~	~~Unfeasible - Too High Per Alt~~
D170B800	170	800	23.147	-139.583	69.023	Desirable - Longest Burn Duration
D170B750	170	750	29.899	-141.016	74.728	Undesirable - High Per Alt
~~D170B700~~	~~170~~	~~700~~	~~39.103~~	~~-143.226~~	~~80.530~~	~~Unfeasible - Too High Per Alt~~
~~D170B600~~	~~170~~	~~600~~	~~81.612~~	~~94.002~~	~~92.411~~	~~Unfeasible - Too High Per Alt, Impact Outside Potential Zone~~

Three of the final trajectory options were eliminated immediately as infeasible; all three yielded final periapsis altitudes that had the potential to skip off the Earth's atmosphere resulting in an uncontrolled and unpredictable reentry. The remaining options were then evaluated against the flight dynamics team's increased understanding of the vehicle and assessment of the various risks involved for each case. Ultimately, case D160B750 was chosen from Table 5 as the option that provided the best chance of a successful deorbit while considering the spacecraft constraints.

Revising the Impact Location

Once the intended maneuver plans for Phase 2 had been adjusted, an additional monte carlo run occurred to create a new impact footprint, shown in Figure 12. The completion of Phase 1 and the reduction in the number of maneuvers to be used in Phase 2 resulted in a more elliptical footprint than the original. The updated monte carlo run yielded a tighter grouping of the impact points due to the reduction in the overall perturbations and the time that the perturbations had to propagate out.

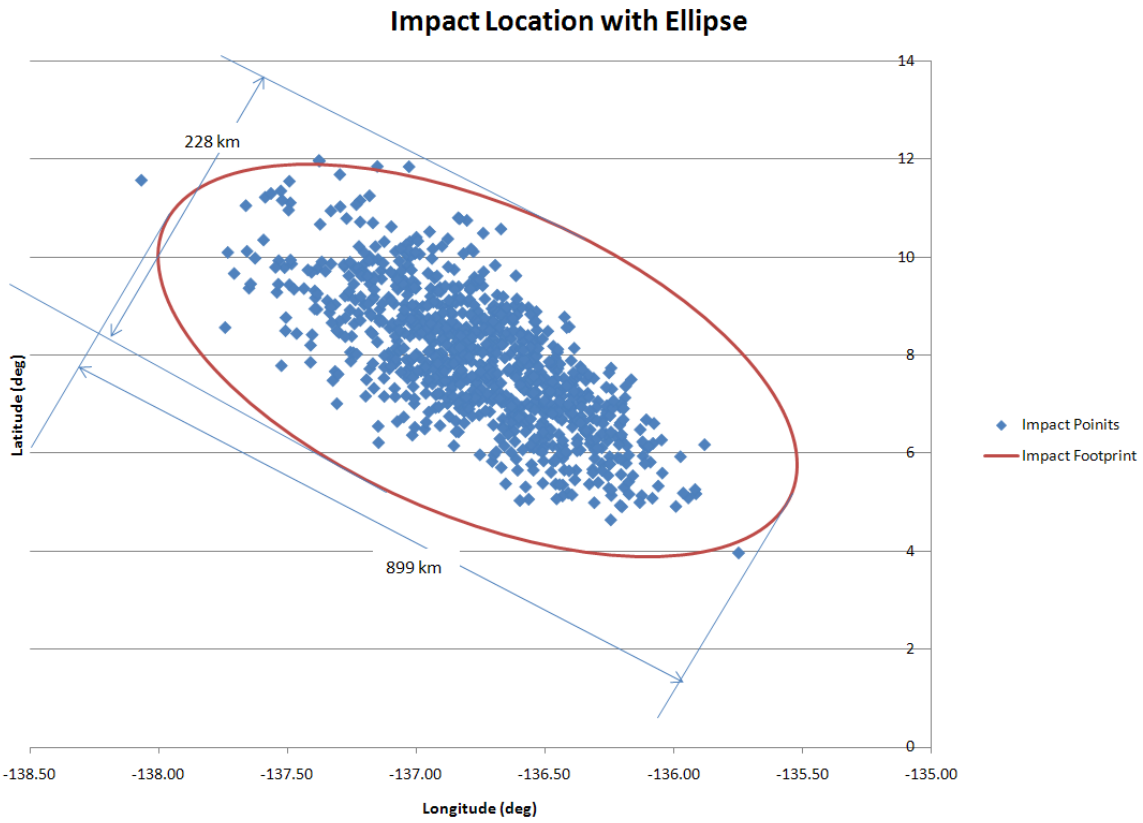

Figure 12. Updated Monte Carlo Impact Locations and 3-Sigma Ellipsoid

Phase 2 Execution

The maneuver results for Phase 2 are shown in Table 6. The first maneuver of Phase 2 ("Maneuver 5") was used to rotate the line of apsides to set the impact location and ensure that the remaining maneuvers were at their optimal location (centered at or near apoapsis). The rotation is illustrated in Figure 13 where there is a change in both periapsis altitude and periapsis altitude, thus rotating the respective locations.

Table 6. Phase 2 Maneuvers Results

Maneuver	Ignition Time (UTCG)	Burn Duration (sec)	Fuel Usage (kg)	Maneuver Goal	Periapsis Alt. (km)	Apoapsis Alt. (km)	Thrust Eff. (%)	Total Fuel Remaining (kg)
Maneuver 5	05 Mar 2011 15:28:03.000	350.2925	1.9470371	Lower Perigee	261.9827754	319.6708421	95.03	14.632963
Maneuver 6	10 Mar 2011 00:17:36.020	--------	2.2469003	Lower Perigee	200.1981534	310.0616746	94.9	12.386063
Maneuver 7	13 Mar 2011 02:21:37.000	--------	----------	Lower Perigee	----------	----------	--------	----------
Maneuver 8	13 Mar 2011 05:15:50.000	--------	----------	Lower Perigee	----------	----------	--------	----------

Figure 13. Phase 2 Execution: Spacecraft Orbit Radius in km

The final maneuver executed on 13 Mar 2011 05:15:50 UTCG and the estimated impact location was centered approximately 3000 miles southeast of the main island of Hawaii (see Figure 14). Telemetry was evaluated throughout Phase 2 and showed the vehicle was healthy and maintaining control prior to Maneuver 8, which led the flight dynamics team to believe that the last maneuver executed successfully. Ultimate confirmation came from JSpOC via Spacetrack where the final satellite TLE released on 14 March listed the object as "Decayed 2011-03-13".

Figure 14. Impact Footprint Location

Maneuver Calibration Evaluation

After each maneuver with sufficient data, a calibration occurred to solve for values characterizing actual thrust efficiency and pointing accuracy. These values were then used as input for the next maneuver (data was not available following the final maneuver of Phase 1 and the last

two maneuvers of Phase 2). The maneuver calibration process utilized a differential corrector method to solve across the maneuver.

The process allows the differential corrector to solve for thrust efficiency and pointing error using the best known information prior to start of the maneuver (updated orbit state, tank pressure), during the maneuver (spacecraft attitude, thruster pulsing, burn duration) and post maneuver (post maneuver orbit state computed from OD). The resulting thrust efficiency and pointing values indicate how closely the maneuver performed compared to the plan and also serve as updates to subsequent maneuver planning.

Table 7, Table 8, Table 9 show the planned and calibrated (actual) values along with the difference between the two. The largest difference occurred for the calibration maneuver. This was due to the limited knowledge regarding the thrusters and their performance before on-orbit data was available. Following the initial calibration, the largest difference occurred for "Maneuver 5" in the tables. The likely cause of this was the longer burn duration where the inefficiencies at the beginning and end of the burn were not as apparent, an effect that was accounted for in the planning of subsequent maneuvers with longer durations.

Table 7. Planned Maneuver Values

Maneuver	Ignition Time (UTCG)	Burn Duration (sec)	Fuel Usage (kg)	Maneuver Goal	Periapsis Alt. (km)	Apoapsis Alt. (km)	Thrust Eff. (%)	Total Fuel Remaining (kg)
Initial State	----------	--------	----------	----------	421.9619479	439.1203476	--------	23.837
Calibration Burn	22 Dec 2010 12:52:34.200	30	0.2062	Lower Perigee	416.3307226	439.0911573	100	23.6308
COLA Mnvr	02 Jan 2011 06:50:32.887	30	0.1884846	Lower Perigee	411.5500685	438.7883065	93.3	23.442315
Maneuver 1	05 Jan 2011 12:27:50.361	296	1.8267387	Lower Perigee	362.4524025	438.3112546	93.3	21.615577
Maneuver 2	07 Jan 2011 13:05:49.722	296	1.7410338	Lower Apogee	363.3822987	390.6765728	92	19.874543
Maneuver 3	09 Jan 2011 14:15:51.466	296	1.6860007	Lower Apogee	343.6878575	364.0669521	92	18.188542
Maneuver 4	11 Jan 2011 17:18:25.000	296	1.6414156	Lower Apogee	319.7440074	342.931244	92	16.547127
Maneuver 5	05 Mar 2011 15:28:03.000	350	1.8861408	Lower Perigee	263.572505	319.6983342	92	14.693859
Maneuver 6	10 Mar 2011 00:17:36.020	418	2.2492243	Lower Perigee	200.0421115	309.9677742	95	12.383776
Maneuver 7	13 Mar 2011 02:21:37.000	264	1.3810163	Lower Perigee	159.9683788	294.689391	95	11.005084
Maneuver 8	13 Mar 2011 05:15:50.000	750	3.6970219	Lower Perigee	64.20942792	292.3669949	93	7.3080781

Table 8. Calibrated Maneuver Values

Maneuver	Ignition Time (UTCG)	Burn Duration (sec)	Fuel Usage (kg)	Maneuver Goal	Periapsis Alt. (km)	Apoapsis Alt. (km)	Thrust Eff. (%)	Total Fuel Remaining (kg)
Initial State	----------	--------	----------	----------	421.9619479	439.1203476	--------	23.837
Calibration Burn	22 Dec 2010 12:52:34.200	30.34775	0.1895	Lower Perigee	416.7681586	439.1076402	93.3	23.6475
COLA Mnvr	02 Jan 2011 06:50:32.887	30.01675	0.186699	Lower Perigee	411.598784	438.78833	94.6	23.460801
Maneuver 1	05 Jan 2011 12:27:50.361	287.705	1.8034532	Lower Perigee	363.0832021	438.311241	92.09	21.657348
Maneuver 2	07 Jan 2011 13:05:49.722	287.7125	1.7469524	Lower Apogee	363.3818341	390.5161209	92.164	19.910395
Maneuver 3	09 Jan 2011 14:15:51.466	286.3125	1.6858694	Lower Apogee	343.7927444	364.0438907	91.727	18.224526
Maneuver 4	11 Jan 2011 17:18:25.000	--------	----------	Lower Apogee	----------	----------	--------	----------
Maneuver 5	05 Mar 2011 15:28:03.000	350.2925	1.9470371	Lower Perigee	261.9827754	319.6708421	95.03	14.632963
Maneuver 6	10 Mar 2011 00:17:36.020	--------	2.2469003	Lower Perigee	200.1981534	310.0616746	94.9	12.386063
Maneuver 7	13 Mar 2011 02:21:37.000	--------	----------	Lower Perigee	----------	----------	--------	----------
Maneuver 8	13 Mar 2011 05:15:50.000	--------	----------	Lower Perigee	----------	----------	--------	----------

Table 9. Planned vs. Calibration Delta Values

Maneuver	Ignition Time (UTCG)	Burn Duration (sec)	Fuel Usage (kg)	Maneuver Goal	Periapsis Alt. (km)	Apoapsis Alt. (km)	Thrust Eff. (%)	Total Fuel Remaining (kg)
Initial State	----------	--------	----------	----------	0	0	--------	0
Calibration Burn	22 Dec 2010 12:52:34.200	0.34775	-0.0167	Lower Perigee	0.437435957	0.016482866	-6.7	0.0167
COLA Mnvr	02 Jan 2011 06:50:32.887	0.01675	-0.0017856	Lower Perigee	0.048715505	2.35267E-05	1.3	0.0017856
Maneuver 1	05 Jan 2011 12:27:50.361	-8.295	-0.0232855	Lower Perigee	0.630799574	-1.362E-05	-1.21	0.0232855
Maneuver 2	07 Jan 2011 13:05:49.722	-8.2875	0.0059186	Lower Apogee	-0.00046465	-0.1604519	0.1638	-0.0059186
Maneuver 3	09 Jan 2011 14:15:51.466	-9.6875	-0.0001313	Lower Apogee	0.104886969	-0.02306144	-0.2734	0.0001313
Maneuver 4	11 Jan 2011 17:18:25.000	--------	----------	Lower Apogee	----------	----------	--------	----------
Maneuver 5	05 Mar 2011 15:28:03.000	0.2925	0.0608963	Lower Perigee	-1.58972957	-0.02749209	3.03	-0.0608963
Maneuver 6	10 Mar 2011 00:17:36.020	--------	-0.002324	Lower Perigee	0.156041982	0.093900355	-0.0999	0.002324
Maneuver 7	13 Mar 2011 02:21:37.000	--------	----------	Lower Perigee	----------	----------	--------	----------
Maneuver 8	13 Mar 2011 05:15:50.000	--------	----------	Lower Perigee	----------	----------	--------	----------

ACKNOWLEDGMENTS

The authors of this paper would like to thank the following people for their dedication, commitment and creativity in the successful deorbit. Mike Bashioum, Sandy Pitzak, David Sipple, Sean LevTov, Mike Mahoney, John Carrico, John Earp, Travis Schrift, Hank Grabowski, Carlos Niederstrasser, Kevin MacMillian, Sudeep Singh, Rob Bowlin, Dave Ward and the countless others.

REFERENCES

[1] T.S Kelso. “CelesTrack” http://celestrack.com/, Dec 19, 2010.

[2] “Process for Limiting Orbital Debris”, NASA-STD 8719.4, 23 July 2009.

[3] Ellipse” Wikipedia, http://en.wikipedia.org/wiki/Ellipse, 19 December 2010.